Recent Advances in Quantifying Wet Scavenging Efficiency of Black Carbon Aerosol

Yuxiang Yang [1,2], Yuzhen Fu [1,2], Qinhao Lin [1], Feng Jiang [1,2], Xiufeng Lian [1,2], Lei Li [3], Zhanyong Wang [4], Guohua Zhang [1,*], Xinhui Bi [1], Xinming Wang [1] and Guoying Sheng [1]

[1] State Key Laboratory of Organic Geochemistry and Guangdong Key Laboratory of Environmental Protection and Resources Utilization, Guangzhou Institute of Geochemistry, Chinese Academy of Sciences, Guangzhou 510640, China; dqhxwlyyx@163.com (Y.Y.); fyzgsby2012@163.com (Y.F.); linqinhao@gig.ac.cn (Q.L.); jiangfengucas@163.com (F.J.); lianxiufeng15@126.com (X.L.); bixh@gig.ac.cn (X.B.); wangxm@gig.ac.cn (X.W.); shenggy@gig.ac.cn (G.S.)

[2] University of Chinese Academy of Sciences, Beijing, 100049, China

[3] Institute of Mass Spectrometer and Atmospheric Environment, Jinan University, Guangzhou 510632, China; lileishdx@163.com

[4] School of Intelligent Systems Engineering, Sun Yat-sen University, Shenzhen 518107, China; wangzy1026@163.com

[*] Correspondence: zhanggh@gig.ac.cn

Abstract: Black carbon (BC) aerosol is of great importance not only for its strong potential in heating air and impacts on cloud, but also because of its hazards to human health. Wet deposition is regarded as the main sink of BC, constraining its lifetime and thus its impact on the environment and climate. However, substantial controversial and ambiguous issues in the wet scavenging processes of BC are apparent in current studies. Despite of its significance, there are only a small number of field studies that have investigated the incorporation of BC-containing particles into cloud droplets and influencing factors, in particular, the in-cloud scavenging, because it was simplicitly considered in many studies (as part of total wet scavenging). The mass scavenging efficiencies (MSEs) of BC were observed to be varied over the world, and the influencing factors were attributed to physical and chemical properties (e.g., size and chemical compositions) and meteorological conditions (cloud water content, temperature, etc.). In this review, we summarized the MSEs and potential factors that influence the in-cloud and below-cloud scavenging of BC. In general, MSEs of BC are lower at low-altitude regions (urban, suburban, and rural sites) and increase with the rising altitude, which serves as additional evidence that atmospheric aging plays an important role in the chemical modification of BC. Herein, higher altitude sites are more representative of free-tropospheric conditions, where BC is usually more aged. Despite of increasing knowledge of BC–cloud interaction, there are still challenges that need to be addressed to gain a better understanding of the wet scavenging of BC. We recommend that more comprehensive methods should be further estimated to obtain high time-resolved scavenging efficiency (SE) of BC, and to distinguish the impact of in-cloud and below-cloud scavenging on BC mass concentration, which is expected to be useful for constraining the gap between field observation and modeling simulation results.

Keywords: black carbon; wet scavenging; scavenging efficiency; aerosol; cloud

1. Introduction

Black carbon (BC), also known as soot or elemental carbon (EC), is primarily produced from incomplete combustion [1]. Approximately 53–57% of BC originates from the combustion of fossil fuel, while the remaining is from biomass burning on a global-scale [2]. BC shows pronounced environmental and climatic effects, including direct radiative forcing and indirect effects. The direct radiative forcing of BC was, only lower than those of carbon dioxide (CO_2) and anthropogenic methane (CH_4) [3]. The indirect effect refers to the change of microphysical and radiative properties of clouds and its lifetime by acting as cloud condensation nuclei (CCN) or ice nuclei (IN) [4–7]. BC is ubiquitous in fog/cloud droplets and ice crystals [8–11], but its ability to serve as CCN/IN remains ambiguous [12], representing a major uncertainty in its climate effect. In mixed-phase or ice cloud, BC may promote the occurrence of precipitation [13]. In tropical areas, BC can even influence the intensity and the location of precipitation [14]. In addition, BC may be harmful or even fatal to humans when inhaled due to its small size and complicated hazardous components [15–20].

Previous studies have shown that there are huge emissions of BC in the world (3132–10,084 Gg yr^{-1}, with a central value of 4626 Gg yr^{-1}), including Europe, South America, Africa, and East China [21,22]. The only sink of BC in atmosphere is dry and wet deposition (or wet scavenging) rather than participation in chemical processes due to its chemically inert nature [23]. On a global-scale, the amount of BC wet scavenging to ocean is fivefold higher than dry deposition [24], and the percentage can even increase to 98% in total deposition in Arctic [25]. BC dramatically promotes warming in Arctic [26], and the deposition on snow and ice surface leads to the reduction of albedo, resulting in the melting of icebergs and further influences the global climate [27–29]. Wet scavenging is also considered to be crucial in the alteration of mixing state and size distribution of BC-containing particles in the atmosphere [30]. Besides, different wet scavenging pathways lead to different mixing states of BC with snow (internal/externally), resulting in different levels of albedo reduction and radiation increasement of snow [31]. A recent study showed that internally mixing of BC–snow reduced the albedo of snow 1.2–2.0 folds more than externally mixing [32]. Given the dependence of the global distribution of BC on long-range transport and deposition, an accurate estimate of wet deposition of BC is thus critical.

While wet deposition is regarded as a major pathway of BC removal in the atmosphere, there are still substantial controversial issues in the mechanisms and controlling factors. Figure 1 illustrates the wet scavenging processes of BC, including in-cloud and below-cloud scavenging. BC can participate in the formation of cloud/fog by acting as CCN, or coagulation/impaction in the cloud. However, BC uptake in clouds is not enough to constitute in-cloud wet scavenging because BC has yet to be scavenged by precipitation, otherwise it can be resuspended by the droplet evaporation and no scavenging took place. Raindrops may subsequently be formed by additional processes, such as coagulation and sublimation if water vapor is sufficient for cloud droplets to grow bigger, namely in-cloud scavenging [33,34]. Raindrops could further scavenge particles via coagulation, impaction, or gravity settling. The part of wet scavenging by raindrops (or other types of precipitation) after leaving the cloud is so-called below-cloud scavenging. In a mixed-phase cloud, the Wegener–Bergeron–Findeisen (WBF) process is of great importance. As illustrated in Figure 1, the water vapor condensed on cloud droplets tends to evaporate and condense again on the surface of ice crystals, for a lower saturation vapor pressure over ice than over liquid water. This process would release a part of BC-containing particles previously incorporated into liquid cloud droplets back to the interstitial phase, which lowers the SE of BC in the liquid phase [35].

The mass scavenging efficiency (MSE) is widely applied to express the in-cloud scavenging ability for aerosols [36]. MSEs of BC were observed to be in a wide range over the world [37–40], and the influencing factors were attributed to physical and chemical properties (e.g., size and chemical compositions) [41,42], and meteorological conditions (cloud water content, temperature, etc.) [43–45]. The ever-changing properties of BC-containing particles throughout their lifetime in the atmosphere and their representation in models could be a major gap between the observations and modeling results [46]. This is mainly attributed to complex aging processes (e.g., coagulation, condensation, and photochemical oxidation), which convert hydrophobic BC to relatively hydrophilic molecules

during atmospheric transport [47,48]. The increase of hygroscopicity can enhance the in-cloud scavenging of BC and thus reduces its lifetime in the atmosphere [49,50].
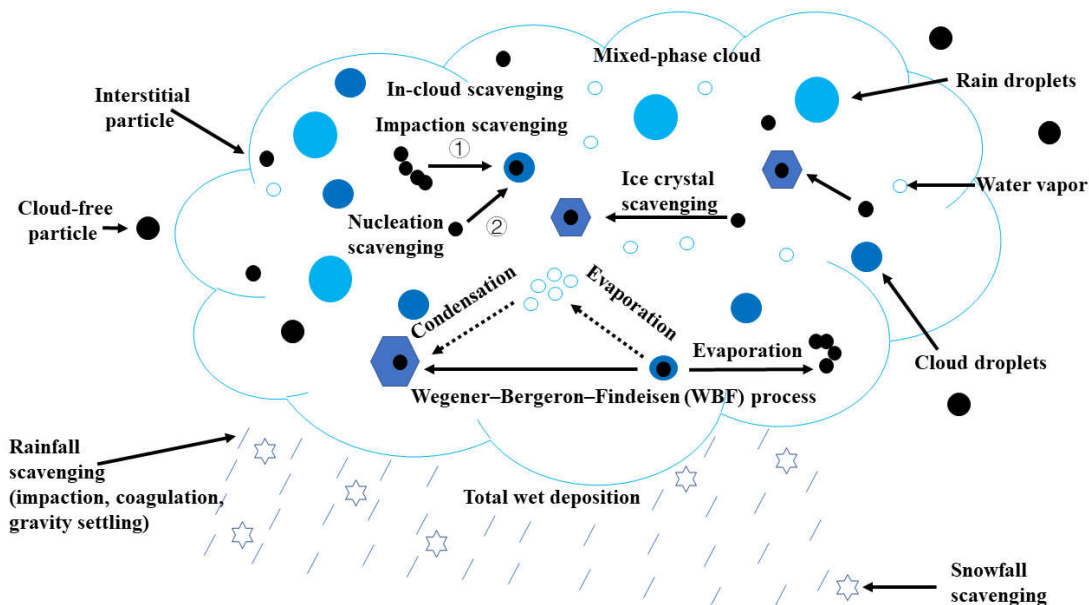

Figure 1. Main processes of wet scavenging of black carbon (BC) (adapted from Hoose et al. [51]).

While numerous studies have focused on the wet scavenging of BC, there is still no comprehensive review specific for this topic. On the other hand, Herckes et al. [36] reviewed the origin, process, and fate of organic matter in cloud/fog. Ervens et al. [52] reviewed the atmospheric processes of various gaseous and particulate species in cloud/fog. In this review paper, we summarize the measurement, scavenging efficiency (SE), and the influencing factors of wet scavenging of BC. The challenges in current studies and perspectives for further studies are also discussed.

2. Methods to Investigate Wet Scavenging of BC

2.1. In-Cloud Scavenging of BC

The SE is defined as the mass/number fraction of BC in cloud droplets, representing the fraction of BC scavenged in-cloud (Equation (1)) [40].

$$\text{SE} = \frac{C_{RES}}{C_{RES} + C_{INT}} \times 100\% \tag{1}$$

Where *SE* refers to MSE or number scavenging efficiency (NSE) and *C_{RES}* and *C_{INT}* denote the mass or number concentration of BC in dried cloud droplet residues and interstitial particles, respectively. During field observations, a counterflow virtual impactor (CVI), ground-based CVI (GCVI), or ice CVI (ICVI) is commonly applied in cloud/fog droplets sampling [53–55]. Briefly, droplets larger than the designated size are introduced into CVI inlet while those below the threshold are excluded by counter flow. Sampled droplets were dried in an evaporation chamber (40 °C), and the resulting residues can be measured by downstream instruments [9]. The mass concentration of BC can be conventionally measured by online instruments such as aethalometer (AE), single particle soot spectrometer (SP2), particle soot/absorption photometer (PSAP), continuous soot monitoring system (COSMOS), and soot particle aerosol mass spectrometer (SP-AMS) [56–60]. The number concentration of BC-containing particle can be quantitively determined by SP2 or semiquantitatively by a single particle mass spectrometer (SPMS) [40,58]. The detailed measurement technologies of

instruments can be found in the related references, so we do not repeat them here; this is the same for those in Section 2.2.

In modeling studies, SE is usually expressed as the scavenging rate constant r (h^{-1}). It is based on the hypothesis that r is in a linear relationship (first-order approximation) with the particle transfer rate into cloud droplets (Equation (2) or its differential form Equation (3)) [61,62].

$$C_t = C_0 \cdot e^{-rt} \tag{2}$$

$$\frac{dC_t}{dt} = -r \cdot C_t \tag{3}$$

Where C_t denotes the instantaneous mass concentration, C_0 stands for the initial mass concentration, and t refers to the cloud processing duration (h).

Liu et al. [63] considered the liquid phase and ice phase separately and expressed the in-cloud scavenging coefficient as Equation (4).

$$F_{in} = F_{prec\,p} \cdot SF_{BC}^*, \quad SF_{BC}^* = \frac{P_{rain} \cdot F_{BC,liq} + P_{snow} \cdot F_{BC,ice}}{P_{rain} + P_{snow}} \tag{4}$$

Where F_{in} denotes the in-cloud scavenging rate (s^{-1}) and $F_{prec\,p}$ is the fractional rate of conversion of cloud droplet into precipitation. SF_{BC}^* denotes the fraction of hydrophilic BC in cloud droplets and ice crystals, and $SF_{BC,liq}$ and $SF_{BC,ice}$ denote the fraction of hydrophilic BC in these two phases, respectively. P_{rain} and P_{snow} refers to the production of rain and snow (kg·m^{-3}·s^{-1}), respectively.

Also, in mixed-phase clouds, WBF process and riming are competitive mechanisms that affecting in-cloud SE of BC, which dominate the SE under different conditions. A global 3-D chemical transport model (GEOS-Chem) had been used to simulate the in-cloud scavenging behaviors in large-scale mixed-phase clouds, in which the expressions of SE were various with riming or WBF effect dominating (Table 4 in Qi et al. [64]).

In addition, some modeling studies explicitly simulate the cloud and aerosol microphysics instead of calculating the scavenging rate constant with a specific formula [65,66]. These simulations may better represent the actual scavenging behaviors in cloud compare to the simple first-order assumption used in Equations (2) or (3).

2.2. Below-Cloud and Total Wet Scavenging of BC

As mentioned above, the total wet scavenging of BC by rainfall includes in-cloud and below-cloud scavenging. However, it is difficult to distinguish below-cloud scavenging from total wet scavenging. Consequently, a modeling simulation becomes a considerable tool to address such issues. Nevertheless, related researches focused on soluble compounds rather than BC [67,68]. Unlike in-cloud scavenging, studies of total wet scavenging were generally fulfilled with offline approaches, which usually require pretreatments, rendering a lower time resolution. BC in rainwater samples are quantified with various methods, including thermal-optical technology (TOT) [69,70], SP2 [58], and ultraviolet–visible spectrophotometer (UV/VIS) [71]. Equation (2) is also compatible when studying the scavenging rate constant (r) in total wet scavenging by rainfall [61,72,73].

Snowfall is another type of precipitation dominating in freezing cold areas. The scavenging ratio is usually defined as the quotient of the mass concentration of BC in snow to that in air (Equation (5)) [74].

$$\omega_S = \frac{C_{snow} \cdot \rho_{air}}{C_{air}} \times 100\% \tag{5}$$

Where ω_s refers to the scavenging ratio of BC by snowfall and C_{snow} (ng g^{-1}) and C_{air} (μg m^{-3}) denote the mass concentration of BC in snow and air, respectively. ρ_{air} is the density of air (1.29 kg m^{-3}). To describe the total wet scavenging of BC more subtly, Hegg et al. [75] expanded this equation by taking the in-cloud SE of BC and precipitation rate into account (Equation (1) in that reference), which have been revealed to be of great essence.

With the intention of describing the total scavenging in a uniform way, washout ratio for snow or rain can also be expressed as Equation (6).

$$r_w = \frac{[BC]_{snow/rain}}{[BC]_{air}} \times 100\% \qquad (6)$$

Where r_w is the washout ratio, while $[BC]_{snow/rain}$ and $[BC]_{air}$ represent the BC mass mixing ratio (concentration) in snow/rain and air, respectively. We did not focus on washout ratios of snow or rain in the following text, since it is only a qualitative index [64], and few studies were available. Given the inherent discrepancies of calculation methods between in-cloud and total wet scavenging, one should be careful to make a comparison between these two kinds of SE.

Recently, Xu et al. [76] described wet scavenging of BC with the conversion rates k (s^{-1}) of BC from one phase to another in wet scavenging process in Community Earth System Model (CESM), including cloud activation, ice nucleation, immersion, contact/homogeneous freezing, riming, and so forth. Since the treatment firstly described most processes that BC may undergo during total wet scavenging in a uniform way, it could be a trend for future modeling study.

3. Current State of Knowledge of Wet Scavenging of BC

3.1. In-Cloud Mass Scavenging Efficiency of BC

Studies of cloud/fog scavenging of BC can be traced back to as early as 1980s [77]. Despite the importance of activation of BC-containing particles into cloud droplets, there have only been a small number of studies that have investigated the CCN activation of BC particles under real atmospheric conditions. Herein, we summarized the published data reporting the in-cloud MSEs of BC in Figure 2, mainly including the results from liquid could/fog investigations. It can be seen that the in-cloud MSE of BC varied in a wide range around the world. For instance, differences can be observed between an urban site (6%) and a rural site (39%) located in the same region (Po Valley, Italy) [78,79]. MSEs are comparable for some regions at similar altitudes, such as Puy de Dôme, Mt. Nanling, and Mt. Sonnblick [37,40,80]. Despite the variability, MSEs of BC are generally lower at low-altitude regions (urban, suburban, and rural sites) and increase with rising altitude ($p < 0.05$). These results might serve as evidence that atmospheric aging plays an important role in the chemical modification of BC, resulting in increased hygroscopicity of BC. Since high-altitude regions (usually background or mountain sites) are far from anthropogenic emission sources, BC-containing particles are likely to be heavily influenced by long-range transportation, and thus become more aged [9]. However, there are also some exceptions. At a remote mid-altitude marine site near Arctic (Zeppelin, Norway), the MSE was extremely high (~80%) [81]. This was explained by the highly aged BC-containing particles from long-range transport. A high MSE (71%) was also observed at a polluted urban site (Ji'nan, China) [82]. It is noted that the reported MSE was only an estimate from the reduction of BC concentration over the fog event, which is different from the calculation with Equation (1) representing a direct measurement result, and thus there might be other influencing factors (such as wind speed) that cannot be excluded in such estimation.
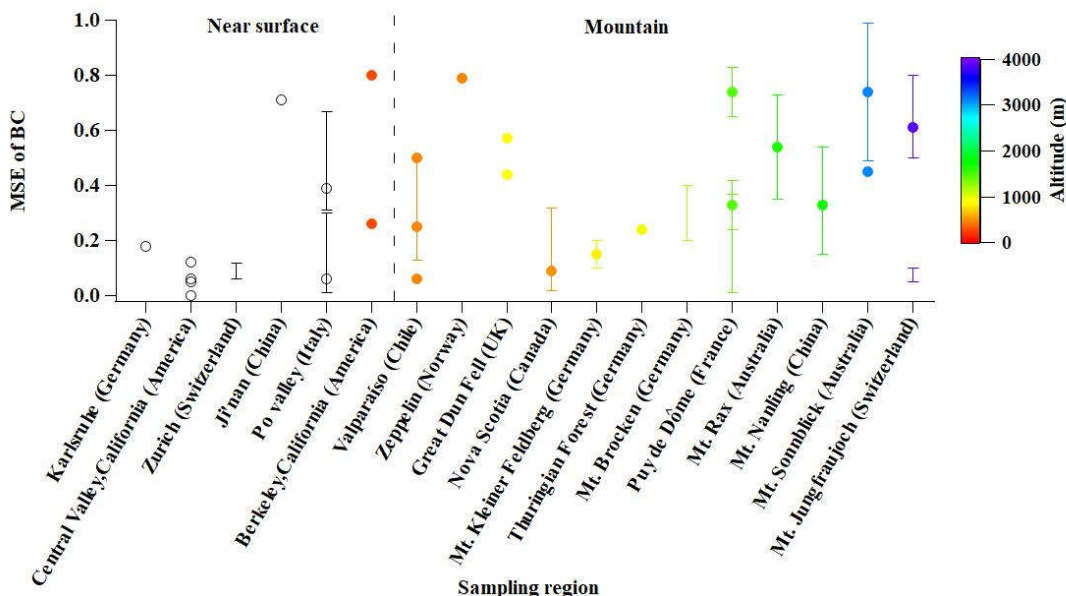
Figure 2. In-cloud mass scavenging efficiency (MSE) of BC (mean or median values with observed ranges) reported in previous literatures, separated for near ground surface and mountain sites. The color scale denotes the altitudes of the sampling sites while the hollow dots denotes no altitude data available. More than one dot for a single site means the SEs were measured under different circumstances (e.g., time [78,79], diameter ranges [37], cloud types [35], air masses [38,83], peak supersaturation [84], etc.). Observational data were collected from Karlsruhe, Germany [85], Central Valley of California, America [86], Zurich, Switzerland [87], Po valley, Italy [78,79], Ji'nan, China [82], Berkeley, California, America [77,88], Valparaíso, Chile [38], Zeppelin, Norway [81], Great Dun Fell, UK [83], Nova Scotia, Canada [89], Mt. Kleiner Feldberg, Germany [90], Thuringian Forest, Germany [91], Mt. Brocken, Germany [92], Mt. Puy de Dôme, France [37,93], Mt. Rax, Australia [43], Mt. Nanling, China [40], Mt. Sonnblick, Australia [80,94], and Mt. Jungfraujoch, Switzerland [35,84].

3.2. Factors that Influence the In-Cloud SE of BC

Various factors, including the diameter of particles, mixing state, the thickness of coating materials and their chemical compositions, the supersaturation of water vapor/ liquid water content (LWC), and so on, have potential impact on the in-cloud SE of BC in liquid cloud [35,39,40,95–97]. Both field observations and model simulations indicated that the SE of BC rises with the increasing particle diameter [37,40,98], in which the coating thickness plays an important role. While it is well-stated that size matters more than chemical compositions [99], the mixing state may play a relatively important role in activation of BC-containing particles. In particular, Matsui [96] found that the mass concentration of BC in interstitial phase would be underestimated by 40–60% when the influence of mixing state was excluded. Schroder et al. [39] found that BC-containing particles with 85-nm cores can only be activated after being coated thicker than 80 nm. Zhang et al. [40] pointed out that mixing state is a key factor that influence the SE of BC under low LWC (< 0.1 g m^{-3}) condition. The internal mixing with sulfate (rather than organic materials) improves the incorporation of BC particles into cloud droplets [40]. Studies have revealed that BC aging timescale directly influences the mixing state of BC and hence BC wet scavenging and global budget [100–102]. He et al. [102] found condensation dominated in particle aging globally (>70%), which facilitates particles to be removed by wet scavenging processes. Through a high time-resolved ambient measurement, a recent work confirmed the fundamental role of the mixing state in determining the hygroscopicity of BC-containing particles [103]. Sarangi et al [104] figured out that mixing state was still a governing factor in the hygroscopicity of Aitken-mode BC-containing particles whose sizes were down to 70 nm. Consistently, BC-containing particles found in cloud droplet residuals were of mixed composition, often having water-soluble coating materials [39,40]. MSE of BC is fairly low (6%) when internally mixed with limited

soluble components in urban environment [78]. The BC coated with inorganic salts (sulfate, nitrate, etc.) are more easily to be removed compare to those coated with organics [40]. The mass/number concentration of BC in mixed-phase cloud could also a potential factor in influencing the SE. Cozic et al. [35] found the MSEs of BC decreases with the increasing mass concentration, resulting in the depletion of available water vapor by considerable available CCN/IN. A considerably high concentration of BC will compete for the limited water vapor, hindering the activation to CCN/IN.

It is well known that water vapor supersaturation has predominant influence in the activation of particles. As is known, it is not likely for freshly emitted BC particles to act as CCN due to their hydrophobicity unless the water vapor supersaturation is higher than 2% [105], far beyond the actual supersaturation (0.1–0.6%) in ambient air [98]. Generally, the half-activated diameter increases with decreasing LWC. Recent study performed at Mt. Jungfraujoch, Switzerland revealed that the MSE of BC of liquid cloud increased from ~50% under peak supersaturation (SS_{peak}) of 0.21% to ~80% under SS_{peak} of 0.5% [84], similar to the modeling results provided by Matsui [96], which showed a soaring MSE of BC from 50–80% at a supersaturation of 0.1% to almost 100% at a supersaturation of 1%.

Ambient temperature is also one of the parameters influencing the SE of BC. Attributed to the WBF process, the MSE of BC generally decreases with decreasing temperature in mixed-phase cloud [35]. The above study also showed that the MSEs of BC were much lower in mixed-phase cloud (5%–10%) than those in liquid-phase cloud (61% on average) [35]. Consistently, the mass concentration of BC was observed to be the highest in interstitial particles, followed by that in liquid and ice phases at Mt. Puy de Dôme site in France [93].

The in-cloud scavenging of BC through acting as IN is considered to be at best moderate [1]. Some studies showed that the depletion of BC in ice crystal by number revealed that BC is nonsignificant in ice crystal formation [12,106]. Similarly, Cziczo et al. [107] showed that BC was essentially absent in ice residue particles in cirrus cloud. However, observations performed at Jungfraujoch, Switzerland found that in the mixed-phase cloud, the mass fraction of BC in the ice crystal (27%) was much higher than that in the bulk aerosol (5%), indicating the possibility for BC-containing particles to be removed by serving as IN [108]. At the same site, Targino et al. [109] pointed out that the impacts of BC on the crystal structure and size may be non-negligible. Aging processes, at odds with that in liquid-phase clouds, may impede ice formation as most IN are insoluble. Maybe fresh BC (uncoated) owns the highest possibility to be scavenged by acting as IN [1]. In such case, aging is not likely to enhance the ability of being scavenged by acting as IN. An exception is with organic coating, which may promote the heterogeneous ice formation [110].

3.3. Total Wet Scavenging of BC by Precipitation

3.3.1. SE of Total BC Wet Scavenging

Rainfall is the most frequent precipitation type of aerosol particles in the atmosphere. A study performed in Arctic highlighted the importance of convective clouds outside the Arctic cycle in improving the total SE of BC [111]. Liu et al. [112] reported that precipitation can remove 65% of BC in the atmosphere at Jungfraujoch, Switzerland. A study carried out in France (temperate zone) and Africa (tropical zone) showed that BC made up 10–72% of carbonaceous particles in rainwater samples [113]. However, these fractions were only 2.5–15% in rainwater and snow water samples at four background sites in Europe, owing to less influence from anthropogenic burning sources [114]. Differences can also be seen in most of Europe (5–25%) and remote areas in Russia and Kazakhstan (30–40%) [115].

Studies focusing on the scavenging of BC by snowfall is rare. Large variability of scavenging ratios (based on Equation (4)) was observed, including the data collected from Mt. Changbai in northeastern China (140 ± 100), Svalbard in Norway (382 and 598 on average at two sites, respectively) and polar regions (98 ± 46 and 69.48 ± 4.79 in different years in the Arctic and 119.54 ± 23.04 in Antarctica), respectively [74,75,116,117]. The variability may be attributed to the uncertainties from the calculation method and complex meteorological conditions [64].

3.3.2. Scavenging of BC by In-Cloud or Below-Cloud Processes

The most pronounced issue in total wet scavenging is the difficulty in distinguishing the contribution of in-cloud and below-cloud scavenging, although they have shown different characteristics in particle scavenging as mentioned above; while the modeling simulation of several precipitation events showed that in-cloud scavenging dominates the total removal above 1000 m (91% of events) and below-cloud scavenging is preferential below 1000 m (52% of events) for bulk aerosol [118]. However, the uncertainties linked to the relative contributions of these mechanisms still needed to be constrained. Recent observational studies also revealed that in-cloud nucleation scavenging is predominant, and controls the wet scavenging efficiency of accumulation-mode aerosols, similar for BC [45,52,119]. Levin et al. [120] found in-cloud nucleation scavenging accounted for 80% removal of particles within a size range of 0.14 to 3.0 μm. Andronache [121] pointed out that the contribution of below-cloud scavenging is negligible compared to in-cloud scavenging for particles within a size range of 0.1 to 1.0 μm under low and moderate rainfall intensity (0.1–10 mm h^{-1}); however, below-cloud scavenging is more efficient to scavenging ultrafine particles (< 0.01 μm) and coarse particles (> 2 μm). In consistent, BC-containing particles were observed to shift to the small sizes with the increasing altitude, reflecting the preferential removal of larger BC-containing particles [122].

Studies on the mass concentrations of BC in rainwater and in air may also give an indication in distinguishing the contribution of in-cloud and below-cloud scavenging. Mori et al. [58] found that the correlation between mass concentrations of BC in rainwater and in air before the precipitation occurred was fairly poor ($R^2 < 0.15$) for a single precipitation event, whereas it increased ($R^2 = 0.58$) when replacing the mass concentration of BC during a single precipitation event with monthly mean value, showing the diversity of total wet scavenging of BC among different precipitation events. A recent study reported a similar phenomenon. In that study, in-cloud scavenging was considered to be the main mechanism of BC removal and the far distance between in-cloud scavenging cloud and the measurement site was the main reason of poor agreement between the mass concentration of BC from precipitation and ambient air [123].

A three-fold higher mass concentration of BC in cloud water compared to that in rainwater in India [124], which might also serve as evidence for the dominant role of in-cloud nucleation scavenging for BC. However, such results are still under debate. A six-year-long field observation conducted in Japan elucidated the decrease of the mass concentration of BC is mainly attributed to below-cloud scavenging rather than in-cloud scavenging [125]. Huo et al. [126] deduced that below-cloud scavenging dominated the BC reduction in highly polluted areas, while in-cloud nucleation determined the SE of BC in clean areas according to the discrepancies of correlation between BC mass concentration and rainfall at urban, suburban and remote sites, respectively.

Potential factors influence the SE of aerosol by precipitation (mostly the below-cloud SE) include the intensity, frequency and duration of rainfall, the mixing process of rainwater and particles, the size distribution of ambient particles and rain droplets, the rain droplets falling velocity, and the category of precipitation [121,127–134]. However, such studies are still limited. Study performed in Lanzhou city, northwestern China revealed that nonthunderstorm rain was more efficient in scavenging particles smaller than 500 nm while thunderstorm was efficient in scavenging particles within 500 to 1000 nm [131]. Heavy rainfall (21.0 mm d^{-1} on average) led to a much higher total wet SE of BC (88% on average) over inland Central China. Modest rainfall (5.0 mm d^{-1} on average) over the East China Sea led to a total wet SE of BC by 47% on average [135]. Kanaya et al. [125] observed a remarkable decrease of ΔBC/ΔCO with the accumulated precipitation, indicating the continuous scavenging of BC by precipitation. In that study, ΔBC/ΔCO was used to characterize the effect of wet scavenging of BC insomuch that wet scavenging shows little influence on the mass concentration of carbon monoxide (CO) compared to BC [136]. Furthermore, Latha et al. [137] built a relationship between the mass concentration of BC and rainfall intensities. They showed that the mass concentration of BC would decrease by 3.6 μg m^{-3} with the each increasement of 1 mm h^{-1} of rainfall intensity in Hyderabad, India. However, one modeling study argued that SE of rainfall may be more sensitive to the frequency of rainfall than intensity of precipitation [133].

3.4. Modeling Results on the Wet Scavenging of BC

Currently, most modeling studies involve in the mass concentration instead of the SE of BC directly. The quantitative comparison of MSE between field observations and modeling simulations can hardly be found, for various uncertainties from environmental conditions [138]. However, the results could still be indicative for the role of wet deposition in the mass concentration of BC in the atmosphere. Using a global chemical transport model, Wang et al. [66] compared mass concentrations of BC particles measured over the central Pacific with the model predictions, and concluded that most models may not be accurately simulating the wet scavenging of BC into cloud droplets. Similarly, Koch et al. [139] compared the simulation mass concentration of BC from various models with measured values on global-scale. The results showed that many models underestimated BC loading in low to mid troposphere in high-latitude areas, which may be linked to the excessive vertical transport and the lack of wet scavenging of BC by precipitation clouds. The comparison between model AeroCom Phase II and observation indicated that put wet scavenging into consideration would shrink the difference between the modeling and observation results, in particular, where the BC mass concentration is dominated by wet scavenging [140]. In the Arctic region, opposite modeling results were obtained. Iversen et al. [141] pointed out the overestimation of precipitation in model led to the underestimation of mass concentration of BC, whereas Browse [44] and Samset et al. [140] showed the opposite results. The underestimation of mass concentration of BC in winter and overestimation in monsoon at four sites in India can be explained by the low emission rate in winter and inefficiency of wet scavenging in monsoon [142].

In the limited studies focusing on the wet scavenging of BC, some modeling results matched well with field observations, reporting similar wet deposition of BC in field observation (72%) and model simulation (60%) in rural areas in East Asia [143,144]. On the other hand, most modeling results disagreed with the field observations. Some researches figured out that taking convective scavenging and coagulation/impaction scavenging into consideration would shrink the gap between modeling simulations and field observations, but large uncertainties still remain [138,145,146]. Currently, most models do not represent in-cloud scavenging processing explicitly, although they do represent total cloud scavenging. In addition, some models do represent in-cloud scavenging with more physical-based parameterizations (e.g., Xu et al. [76], Croft et al. [147], Yang et al. [148]). However, it is still far from sufficient to represent both the in-cloud and below-cloud scavenging of BC. Vignati et al. [46] reported that the lifetime of BC will increase by 10% if the SE of large-scale convectional precipitation decreases by 30%, however, the lifetime would be little changed if no below-scavenging occurs. The underestimation of wet scavenging of BC by snowfall in Canada by two folds in warm cloud and one hundred folds in cold cloud revealed the inflexibility of model, and highlighted the remarkable effectiveness by warm cloud on wet scavenging of BC [149].

4. Research Needs

A number of assumptions on atmospheric processes about BC, which may influence its scavenging behavior, such as the fraction of hydrophilic BC in total BC, time of the transformation from hydrophobic BC into hydrophilic ones, mixing state, and the fraction of hydrophobic BC serving as IN, have been put forward and tested in models. However, these assumptions could not be extensively applicable worldwide [64]. To help better constrain these models, additional studies on the activation of BC into cloud droplets under real atmospheric conditions would be helpful to improve the parameterization in models [150–152].

To parameterize the wet scavenging rate, Equations (2) and (3)$_{\text{Equation (2); Equation (3)}}$ are commonly used. However, they are based on the hypothesis stated in Section 2.1, which simplified the actual scavenging processes. Up to date parameters that are able to describe the wet scavenging of BC are still limited [141,153]. Several studies treated such issues by introducing the parameters used in dry deposition of BC or simply regarding bulk aerosol as a homogenously entirety (including BC). In that case, the parameters are treated as constants, which is not reasonable [21,45,51,143]. Field observations should include critical influencing factors to establish a robust relationship between the SE of BC and the various influence factors. Regarding the certain influence of size and mixing state

on the SE of BC, it is thus critical for modeling studies to include the size-resolved mixing state of BC-containing particles [98,154].

4.1. More Field Measurements on the Direct Links between SEs of BC and the Physical and Chemical Properties of BC-Containing Particles

While there were some separated studies measuring the SEs of BC and the physical and chemical properties of BC-containing particles, knowledge on their direct links are still limited [9,42]. Thus it is necessary to simultaneously investigate the evolution of BC in cloud processes and its interactions with cloud scavenging [87], in order to gain a better understanding on the interactions between BC and clouds. As widely accepted, the physical and chemical properties of BC-containing particles are ever-changing throughout their lifetime in the atmosphere, significantly contributing to the uncertainty associated with the BC–cloud interaction. Size and mixing state are known to be crucial in influencing the lifetime of BC via nucleation scavenging [87,155]. Recent studies have described the size and mixing state of BC with other substances in cloud droplets with SPMS, transmission electron microscopy (TEM), or SP2 [8,11,39,40]. Furthermore, such studies were mostly performed in urban environment [156–158].

Morphology of BC has also been reported to be an ever-changing property in atmospheric processes and show great impacts on climate [159,160]. TEM analysis is an offline approach widely used to observe the morphology of particles [161]. However, few studies have been carried out to describe the morphology of BC in cloud processes. Ueda et al. [162] revealed that most BC-containing particles remained in interstitial phase were insoluble according to the discrepancies of the morphology of BC before and after dialysis with water. Liu et al. [11] used TEM to recognize the morphology and chemical composition of cloud residue particles at Mt. Tai and pointed out that BC incorporated into cloud droplets were attached with sulfate-rich (S-rich) particles, similar to the results for Mt. Nanling site [40].

4.2. High Time-Resolved Investigations of the NSE of BC-Containing Particles

While previous studies reporting MSE of BC could be useful for validating modeling results, the CCN/IN properties of BC-containing particles are more closely linked to particle number concentration and size. However, there were only a small number of studies that have investigated the activation of BC particles into cloud droplets based on particle number concentrations under real atmospheric conditions. In addition, studies investigating BC mass scavenging would miss the information on the contribution of particle size and mixing state to the activation of BC-containing particles into fog/clouds [39,40]. Croft et al. [163] found that the coagulation/impaction scavenging of interstitial particles into larger cloud droplets strongly limited the number concentration of smaller particles (<200 nm). Taking this mechanism into account, the number concentration of cloud droplets larger than 10 nm decreased by 15–21% globally [146]. Based on a two-year-long observation, Yin et al. [164] revealed a moderate correlation between LWC and number concentration of cloud droplets (R = 0.65). Scohroder et al. [39] found the NSE was only 1–10% for BC at Mt. Jungfraujoch. Zhang et al. [40] reported a NSE of 5–45% for BC-containing particles at Mt. Nanling in Southern China, increasing with the increasing particle sizes.

However, there is still no data reporting the high time-resolved NSE of the BC-containing particles. In fact, the life cycle of cloud/fog can be roughly divided into four stages including formation, development, stability and dissipation [165,166]. The physicochemical properties of cloud droplets keep changing in the whole process. The regularity of SE of aerosol particles was not identical even in a cloud event, as observed at the Mt. Åreskutan in Swedish [167].

Abbreviations: Aethalometer (AE); black carbon (BC); cloud condensation nuclei (CCN); methane (CH_4); carbon monoxide (CO); carbon dioxide (CO_2); Community Earth System Model (CESM); continuous soot monitoring system (COSMOS); counterflow virtual impactor (CVI); elemental carbon (EC); ground-based CVI (GCVI); ice CVI (ICVI); ice nuclei (IN); liquid water content (LWC); mass scavenging efficiency (MSE); number scavenging efficiency (NSE); particle soot/absorption photometer (PSAP); scavenging efficiency (SE); soot particle aerosol mass spectrometer (SP-AMS); single particle mass spectrometer (SPMS); single particle soot spectrometer (SP2); supersaturation (SS); peak supersaturation (SS_{peak}); transmission electron microscopy (TEM); thermal-optical technology (TOT); ultraviolet–visible spectrophotometer (UV/VIS); Wegener–Bergeron–Findeisen (WBF).

References

1. Bond, T.C.; Doherty, S.J.; Fahey, D.W.; Forster, P.M.; Berntsen, T.; DeAngelo, B.J.; Flanner, M.G.; Ghan, S.; Kärcher, B.; Koch, D.; et al. Bounding the role of black carbon in the climate system: A scientific assessment. *J. Geophys. Res. Atmos.* **2013**, *118*, 5380–5552, doi:10.1002/jgrd.50171.

2. Liousse, C.; Penner, J.E.; Chuang, C.; Walton, J.J.; Eddleman, H.; Cachier, H. A global three-dimensional model study of carbonaceous aerosols. *J. Geophys. Res. Atmos.* **1996**, *101*, 19411–19432, doi:10.1029/95jd03426.

3. Intergovernmental Panel on Climate Change (IPCC). The Physical Science Basis. In *Contribution of Working Group I to Fifth Assessment Report of the Intergovernmental Panel on Climate Change*; Stocker, T.F., Qin, D., Plattner, G.-K.; Tignor, M., Allen, S.K.; Boschung, J.; Nauels, A.; Xia, Y.; Bex, V.; Midgley, P.M., Eds.; Cambridge University Press: Cambridge, UK, 2013.

4. Koch, D.; Del Genio, A.D. Black carbon semi-direct effects on cloud cover: review and synthesis. *Atmos. Chem. Phys.* **2010**, *10*, 7685–7696, doi:10.5194/acp-10-7685-2010.

5. Conant, W.C.; Nenes, A.; Seinfeld, J.H. Black carbon radiative heating effects on cloud microphysics and implications for the aerosol indirect effect—1. Extended Kohler theory. *J. Geophys. Res. Atmos.* **2002**, *107*, AAC 23-21–AAC 23-29, doi:10.1029/2002jd002094.

6. Nenes, A.; Conant, W.C.; Seinfeld, J.H. Black carbon radiative heating effects on cloud microphysics and implications for the aerosol indirect effect—2. Cloud microphysics. *J. Geophys. Res. Atmos.* **2002**, *107*, AAC 24-21–AAC 24-11, doi:10.1029/2002jd002101.

7. Jacobson, M.Z. Effects of externally-through-internally-mixed soot inclusions within clouds and precipitation on global climate. *J. Phys. Chem. A* **2006**, *110*, 6860–6873, doi:10.1021/jp056391r.

8. Lin, Q.; Zhang, G.; Peng, L.; Bi, X.; Wang, X.; Brechtel, F.J.; Li, M.; Chen, D.; Peng, P.; Sheng, G.; et al. In situ chemical composition measurement of individual cloud residue particles at a mountain site, southern China. *Atmos. Chem. Phys.* **2017**, *17*, 8473–8488, doi:10.5194/acp-17-8473-2017.

9. Bi, X.; Lin, Q.; Peng, L.; Zhang, G.; Wang, X.; Brechtel, F.J.; Chen, D.; Li, M.; Peng, P.; Sheng, G.; et al. In situ detection of the chemistry of individual fog droplet residues in the Pearl River Delta region, China. *J. Geophys. Res. Atmos.* **2016**, *121*, 9105–9116, doi:10.1002/2016jd024886.

10. Levin, E.J.T.; McMeeking, G.R.; DeMott, P.J.; McCluskey, C.S.; Carrico, C.M.; Nakao, S.; Jayarathne, T.; Stone, E.A.; Stockwell, C.E.; Yokelson, R.J.; et al. Ice-nucleating particle emissions from biomass combustion and the potential importance of soot aerosol. *J. Geophys. Res. Atmos.* **2016**, *121*, 5888–5903, doi:10.1002/2016jd024879.

11. Liu, L.; Zhang, J.; Xu, L.; Yuan, Q.; Huang, D.; Chen, J.; Shi, Z.; Sun, Y.; Fu, P.; Wang, Z.; et al. Cloud scavenging of anthropogenic refractory particles at a mountain site in North China. *Atmos. Chem. Phys.* **2018**, *18*, 14681–14693, doi:10.5194/acp-18-14681-2018.

12. Vergara-Temprado, J.; Holden, M.A.; Orton, T.R.; O'Sullivan, D.; Umo, N.S.; Browse, J.; Reddington, C.; Baeza-Romero, M.T.; Jones, M.J.; Lea-Langton, A.; et al. Is Black Carbon an Unimportant Ice-Nucleating Particle in Mixed-Phase Clouds? *J. Geophys. Res. Atmos.* **2018**, *123*, 4273–4283, doi:10.1002/2017JD027831.

13. Lohmann, U. A glaciation indirect aerosol effect caused by soot aerosols. *Geophys. Res. Lett.* **2002**, *29*, 11, doi:10.1029/2001gl014357.

14. Wang, C. A modeling study on the climate impacts of black carbon aerosols. *J. Geophys. Res. Atmos.* **2004**, *109*, doi:10.1029/2003jd004084.

15. Poschl, U. Atmospheric aerosols: composition, transformation, climate and health effects. *Angew. Chem. Int. Ed. Engl.* **2005**, *44*, 7520–7540, doi:10.1002/anie.200501122.

16. Highwood, E.J.; Kinnersley, R.P. When smoke gets in our eyes: the multiple impacts of atmospheric black carbon on climate, air quality and health. *Environ. Int.* **2006**, *32*, 560–566, doi:10.1016/j.envint.2005.12.003.

17. Luben, T.J.; Nichols, J.L.; Dutton, S.J.; Kirrane, E.; Owens, E.O.; Datko-Williams, L.; Madden, M.; Sacks, J.D. A systematic review of cardiovascular emergency department visits, hospital admissions and mortality associated with ambient black carbon. *Environ. Int.* **2017**, *107*, 154–162, doi:10.1016/j.envint.2017.07.005.

18. Geng, F.; Hua, J.; Mu, Z.; Peng, L.; Xu, X.; Chen, R.; Kan, H. Differentiating the associations of black carbon and fine particle with daily mortality in a Chinese city. *Environ. Res.* **2013**, *120*, 27–32, doi:10.1016/j.envres.2012.08.007.

19. Nichols, J.L.; Owens, E.O.; Dutton, S.J.; Luben, T.J. Systematic review of the effects of black carbon on cardiovascular disease among individuals with pre-existing disease. *Int. J. Public Health* **2013**, *58*, 707–724, doi:10.1007/s00038-013-0492-z.

20. Fu, H.; Chen, J. Formation, features and controlling strategies of severe haze-fog pollutions in China. *Sci. Total Environ.* **2017**, *578*, 121–138, doi:10.1016/j.scitotenv.2016.10.201.

21. Cooke, W.F.; Liousse, C.; Cachier, H.; Feichter, J. Construction of a 1° × 1° fossil fuel emission data set for carbonaceous aerosol and implementation and radiative impact in the ECHAM4 model. *J. Geophys. Res. Atmos.* **1999**, *104*, 22137–22162, doi:10.1029/1999jd900187.

22. Bond, T.C.; Streets, D.G.; Yarber, K.F.; Nelson, S.M.; Woo, J.H.; Klimont, Z. A technology-based global inventory of black and organic carbon emissions from combustion. *J. Geophys. Res. Atmos.* **2004**, 109, doi:10.1029/2003jd003697.

23. Seinfeld, J.H.; Pandis, S.N. *Atmospheric Chemistry and Physics: From Air Pollution to Climate Change*, 2nd ed.; Wiley and Sons: Hoboken, NJ, USA, 2006; pp. 60–61, IBSN 978-0-471-72018-8.

24. Jurado, E.; Dachs, J.; Duarte, C.M.; Simo, R. Atmospheric deposition of organic and black carbon to the global oceans. *Atmos. Environ.* **2008**, *42*, 7931–7939, doi:10.1016/j.atmosenv.2008.07.029.

25. Bourgeois, Q.; Bey, I. Pollution transport efficiency toward the Arctic: Sensitivity to aerosol scavenging and source regions. *J. Geophys. Res. Atmos.* **2011**, *116*, doi:10.1029/2010jd015096.

26. Ding, M.; Tian, B.; Zhang, T.; Tang, J.; Peng, H.; Bian, L.; Sun, W. Shipborne observations of atmospheric black carbon aerosol from Shanghai to the Arctic Ocean during the 7th Chinese Arctic Research Expedition. *Atmos. Res.* **2018**, *210*, 34–40, doi:10.1016/j.atmosres.2018.04.016.

27. Tedesco, M.; Doherty, S.; Fettweis, X.; Alexander, P.; Jeyaratnam, J.; Stroeve, J. The darkening of the Greenland ice sheet: trends, drivers, and projections (1981–2100). *Cryosphere* **2016**, *10*, 477–496, doi:10.5194/tc-10-477-2016.

28. Qi, L.; Li, Q.; Li, Y.; He, C. Factors controlling black carbon distribution in the Arctic. *Atmos. Chem. Phys.* **2017**, *17*, 1037–1059, doi:10.5194/acp-17-1037-2017.

29. Ikeda, K.; Tanimoto, H.; Sugita, T.; Akiyoshi, H.; Kanaya, Y.; Zhu, C.; Taketani, F. Tagged tracer simulations of black carbon in the Arctic: transport, source contributions, and budget. *Atmos. Chem. Phys.* **2017**, *17*, 10515–10533, doi:10.5194/acp-17-10515-2017.

30. Miyakawa, T.; Oshima, N.; Taketani, F.; Komazaki, Y.; Yoshino, A.; Takami, A.; Kondo, Y.; Kanaya, Y. Alteration of the size distributions and mixing states of black carbon through transport in the boundary layer in east Asia. *Atmos. Chem. Phys.* **2017**, *17*, 5851–5864, doi:10.5194/acp-17-5851-2017.

31. Liou, K.N.; Takano, Y.; He, C.; Yang, P.; Leung, L.R.; Gu, Y.; Lee, W.L. Stochastic parameterization for light absorption by internally mixed BC/dust in snow grains for application to climate models. *J. Geophys. Res. Atmos.* **2014**, *119*, 7616–7632, doi:10.1002/2014jd021665.

32. He, C.; Liou, K.N.; Takano, Y.; Yang, P.; Qi, L.; Chen, F. Impact of Grain Shape and Multiple Black Carbon Internal Mixing on Snow Albedo: Parameterization and Radiative Effect Analysis. *J. Geophys. Res. Atmos.* **2018**, *123*, 1253–1268, doi:10.1002/2017jd027752.

33. Furutani, H.; Dall'osto, M.; Roberts, G.C.; Prather, K.A. Assessment of the relative importance of atmospheric aging on CCN activity derived from field observations. *Atmos. Environ.* **2008**, *42*, 3130–3142, doi:10.1016/j.atmosenv.2007.09.024.

34. Baumgardner, D.; Subramanian, R.; Twohy, C.; Stith, J.; Kok, G. Scavenging of black carbon by ice crystals over the northern Pacific. *Geophys. Res. Lett.* **2008**, *35*, doi:10.1029/2008gl035764.

35. Cozic, J.; Verheggen, B.; Mertes, S.; Connolly, P.; Bower, K.; Petzold, A.; Baltensperger, U.; Weingartner, E. Scavenging of black carbon in mixed phase clouds at the high alpine site Jungfraujoch. *Atmos. Chem. Phys.* **2007**, *7*, 1797–1807, doi:10.5194/acp-7-1797-2007.

36. Herckes, P.; Valsaraj, K.T.; Collett, J.L., Jr. A review of observations of organic matter in fogs and clouds: Origin, processing and fate. *Atmos. Res.* **2013**, *132*, 434–449, doi:10.1016/j.atmosres.2013.06.005.

37. Sellegri, K.; Laj, P.; Dupuy, R.; Legrand, M.; Preunkert, S.; Putaud, J.P. Size-dependent scavenging efficiencies of multicomponent atmospheric aerosols in clouds. *J. Geophys. Res. Atmos.* **2003**, *108*, doi:10.1029/2002JD002749.

38. Heintzenberg, J.; Cereceda-Balic, F.; Vidal, V.; Leck, C. Scavenging of black carbon in Chilean coastal fogs. *Sci. Total. Environ.* **2016**, *541*, 341–347, doi:10.1016/j.scitotenv.2015.09.057.

39. Schroder, J.C.; Hanna, S.J.; Modini, R.L.; Corrigan, A.L.; Kreidenweis, S.M.; Macdonald, A.M.; Noone, K.J.; Russell, L.M.; Leaitch, W.R.; Bertram, A.K. Size-resolved observations of refractory black carbon particles in cloud droplets at a marine boundary layer site. *Atmos. Chem. Phys.* **2015**, *15*, 1367–1383, doi:10.5194/acp-15-1367-2015.

40. Zhang, G.; Lin, Q.; Peng, L.; Bi, X.; Chen, D.; Li, M.; Li, L.; Brechtel, F.J.; Chen, J.; Yan, W.; et al. The single-particle mixing state and cloud scavenging of black carbon: a case study at a high-altitude mountain site in southern China. *Atmos. Chem. Phys.* **2017**, *17*, 14975–14985, doi:10.5194/acp-17-14975-2017.

41. Ma, Y.; Li, S.; Zheng, J.; Khalizov, A.; Wang, X.; Wang, Z.; Zhou, Y. Size-resolved measurements of mixing state and cloud-nucleating ability of aerosols in Nanjing, China. *J. Geophys. Res. Atmos.* **2017**, *122*, 9430–9450, doi:10.1002/2017jd026583.

42. Liu, D.; Allan, J.; Whitehead, J.; Young, D.; Flynn, M.; Coe, H.; McFiggans, G.; Fleming, Z.L.; Bandy, B. Ambient black carbon particle hygroscopic properties controlled by mixing state and composition. *Atmos. Chem. Phys.* **2013**, *13*, 2015–2029, doi:10.5194/acp-13-2015-2013.

43. Hitzenberger, R.; Berner, A.; Glebl, H.; Drobesch, K.; Kasper-Giebl, A.; Loeflund, M.; Urban, H.; Puxbaum, H. Black carbon (BC) in alpine aerosols and cloud water—concentrations and scavenging efficiencies. *Atmos. Environ.* **2001**, *35*, 5135–5141, doi:10.1016/S1352-2310(01)00312-0.

44. Browse, J.; Carslaw, K.S.; Arnold, S.R.; Pringle, K.; Boucher, O. The scavenging processes controlling the seasonal cycle in Arctic sulphate and black carbon aerosol. *Atmos. Chem. Phys.* **2012**, *12*, 6775–6798, doi:10.5194/acp-12-6775-2012.

45. Ohata, S.; Moteki, N.; Mori, T.; Koike, M.; Kondo, Y. A key process controlling the wet removal of aerosols: new observational evidence. *Sci. Rep.* **2016**, *6*, 34113, doi:10.1038/srep34113.

46. Vignati, E.; Karl, M.; Krol, M.; Wilson, J.; Stier, P.; Cavalli, F. Sources of uncertainties in modelling black carbon at a global scale. *Atmos. Chem. Phys.* **2010**, *10*, 2595–2611.

47. Johnson, K.S.; Zuberi, B.; Molina, L.T.; Molina, M.J.; Cowin, J.P.; Gaspar, D.J.; Wang, C.; Laskin, A. Processing of soot in an urban environment: case study from the Mexico City Metropolitan Area. *Atmos. Chem. Phys.* **2005**, *5*, 3033–3043.

48. Zhang, R.; Khalizov, A.F.; Pagels, J.; Zhang, D.; Xue, H.; McMurry, P.H. Variability in morphology, hygroscopicity, and optical properties of soot aerosols during atmospheric processing. *Proc. Natl. Acad. Sci. USA* **2008**, *105*, 10291–10296, doi:10.1073/pnas.0804860105.

49. Zaveri, R.A.; Barnard, J.C.; Easter, R.C.; Riemer, N.; West, M. Particle-resolved simulation of aerosol size, composition, mixing state, and the associated optical and cloud condensation nuclei activation properties in an evolving urban plume. *J. Geophys. Res. Atmos.* **2010**, *115*, doi:10.1029/2009JD013616.

50. Henning, S.; Ziese, M.; Kiselev, A.; Saathoff, H.; Mohler, O.; Mentel, T.F.; Buchholz, A.; Spindler, C.; Michaud, V.; Monier, M.; et al. Hygroscopic growth and droplet activation of soot particles: uncoated, succinic or sulfuric acid coated. *Atmos. Chem. Phys.* **2012**, *12*, 4525–4537, doi:10.5194/acp-12-4525-2012.

51. Hoose, C.; Lohmann, U.; Bennartz, R.; Croft, B.; Lesins, G. Global simulations of aerosol processing in clouds. *Atmos. Chem. Phys.* **2008**, *8*, 6939–6963, doi:10.5194/acp-8-6939-2008.

52. Ervens, B. Modeling the processing of aerosol and trace gases in clouds and fogs. *Chem. Rev.* **2015**, *115*, 4157–4198, doi:10.1021/cr5005887.

53. Mertes, S.; Verheggen, B.; Walter, S.; Connolly, P.; Ebert, M.; Schneider, J.; Bower, K.N.; Cozic, J.; Weinbruch, S.; Baltensperger, U.; et al. Counterflow Virtual Impactor Based Collection of Small Ice Particles in Mixed-Phase Clouds for the Physico-Chemical Characterization of Tropospheric Ice Nuclei: Sampler Description and First Case Study. *Aerosol Sci. Technol.* **2007**, *41*, 848–864, doi:10.1080/02786820701501881.

54. Shingler, T.; Dey, S.; Sorooshian, A.; Brechtel, F.J.; Wang, Z.; Metcalf, A.; Coggon, M.; Mulmenstadt, J.; Russell, L.M.; Jonsson, H.H.; et al. Characterisation and airborne deployment of a new counterflow virtual impactor inlet. *Atmos. Meas. Tech.* **2012**, *5*, 1259–1269, doi:10.5194/amt-5-1259-2012.

55. Sorooshian, A.; Wang, Z.; Coggon, M.M.; Jonsson, H.H.; Ervens, B. Observations of sharp oxalate reductions in stratocumulus clouds at variable altitudes: organic acid and metal measurements during the 2011 E-PEACE campaign. *Environ. Sci. Technol.* **2013**, *47*, 7747–7756, doi:10.1021/es4012383.

56. Petzold, A.; Ogren, J.A.; Fiebig, M.; Laj, P.; Li, S.; Baltensperger, U.; Holzer-Popp, T.; Kinne, S.; Pappalardo, G.; Sugimoto, N.; et al. Recommendations for reporting "black carbon" measurements. *Atmos. Chem. Phys.* **2013**, *13*, 8365–8379, doi:10.5194/acp-13-8365-2013.

57. Drinovec, L.; Močnik, G.; Zotter, P.; Prévôt, A.S.H.; Ruckstuhl, C.; Coz, E.; Rupakheti, M.; Sciare, J.; Müller, T.; Wiedensohler, A.; et al. The "dual-spot" Aethalometer: an improved measurement of aerosol black carbon with real-time loading compensation. *Atmos. Meas. Tech.* **2015**, *8*, 1965–1979, doi:10.5194/amt-8-1965-2015.

58. Mori, T.; Kondo, Y.; Ohata, S.; Moteki, N.; Matsui, H.; Oshima, N.; Iwasaki, A. Wet deposition of black carbon at a remote site in the East China Sea. *J. Geophys. Res. Atmos.* **2014**, *119*, 10485–10498, doi:10.1002/2014jd022103.

59. Wang, J.; Zhang, Q.; Chen, M.; Collier, S.; Zhou, S.; Ge, X.; Xu, J.; Shi, J.; Xie, C.; Hu, J.; et al. First Chemical Characterization of Refractory Black Carbon Aerosols and Associated Coatings over the Tibetan Plateau (4730 m a.s.l). *Environ. Sci. Technol.* **2017**, *51*, 14072–14082, doi:10.1021/acs.est.7b03973.

60. Sinha, P.R.; Kondo, Y.; Koike, M.; Ogren, J.A.; Jefferson, A.; Barrett, T.E.; Sheesley, R.J.; Ohata, S.; Moteki, N.; Coe, H.; et al. Evaluation of ground-based black carbon measurements by filter-based photometers at two Arctic sites. *J. Geophys. Res. Atmos.* **2017**, *122*, 3544–3572, doi:10.1002/2016jd025843.

61. Bae, S.Y.; Jung, C.H.; Kim, Y.P. Relative contributions of individual phoretic effect in the below-cloud scavenging process. *J. Aerosol Sci.* **2009**, *40*, 621–632, doi:10.1016/j.jaerosci.2009.03.003.

62. Wang, Z.; Wang, T.; Guo, J.; Gao, R.; Xue, L.; Zhang, J.; Zhou, Y.; Zhou, X.; Zhang, Q.; Wang, W. Formation of secondary organic carbon and cloud impact on carbonaceous aerosols at Mount Tai, North China. *Atmos. Environ.* **2012**, *46*, 516–527, doi:10.1016/j.atmosenv.2011.08.019.

63. Liu, J.; Fan, S.; Horowitz, L.W.; Levy, H. Evaluation of factors controlling long-range transport of black carbon to the Arctic. *J. Geophys. Res. Atmos.* **2011**, 116, doi:10.1029/2010jd015145.

64. Qi, L.; Li, Q.; He, C.; Wang, X.; Huang, J. Effects of the Wegener–Bergeron–Findeisen process on global black carbon distribution. *Atmos. Chem. Phys.* **2017**, *17*, 7459–7479, doi:10.5194/acp-17-7459-2017.

65. Chen, X.; Wang, Z.; Yu, F.; Pan, X.; Li, J.; Ge, B.; Wang, Z.; Hu, M.; Yang, W.; Chen, H. Estimation of atmospheric aging time of black carbon particles in the polluted atmosphere over central-eastern China using microphysical process analysis in regional chemical transport model. *Atmos. Environ.* **2017**, *163*, 44–56, doi:10.1016/j.atmosenv.2017.05.016.

66. Wang, Q.; Jacob, D.J.; Spackman, J.R.; Perring, A.E.; Schwarz, J.P.; Moteki, N.; Marais, E.A.; Ge, C.; Wang, J.; Barrett, S.R.H. Global budget and radiative forcing of black carbon aerosol: Constraints from pole-to-pole (HIPPO) observations across the Pacific. *J. Geophys. Res. Atmos.* **2014**, *119*, 195–206, doi:10.1002/2013jd020824.

67. Xu, D.; Ge, B.; Wang, Z.; Sun, Y.; Chen, Y.; Ji, D.; Yang, T.; Ma, Z.; Cheng, N.; Hao, J.; et al. Below-cloud wet scavenging of soluble inorganic ions by rain in Beijing during the summer of 2014. *Environ. Pollut.* **2017**, *230*, 963–973, doi:10.1016/j.envpol.2017.07.033.

68. Aikawa, M.; Kajino, M.; Hiraki, T.; Mukai, H. The contribution of site to washout and rainout: Precipitation chemistry based on sample analysis from 0.5 mm precipitation increments and numerical simulation. *Atmos. Environ.* **2014**, *95*, 165–174, doi:10.1016/j.atmosenv.2014.06.015.

69. Hadley, O.L.; Corrigan, C.E.; Kirchstetter, T.W. Modified Thermal-Optical Analysis Using Spectral Absorption Selectivity to Distinguish Black Carbon from Pyrolyzed Organic Carbon. *Environ. Sci. Technol.* **2008**, *42*, 8459–8464, doi:10.1021/es800448n.

70. Zhao, S.; Chen, L.; Yan, J.; Shi, P.; Li, Y.; Li, W. Characteristics of Particulate Carbon in Precipitation during the Rainy Season in Xiamen Island, China. *Atmosphere* **2016**, *7*, 140, doi:10.3390/atmos7110140.

71. Torres, A.; Bond, T.C.; Lehmann, C.M.B.; Subramanian, R.; Hadley, O.L. Measuring Organic Carbon and Black Carbon in Rainwater: Evaluation of Methods. *Aerosol Sci. Tech.* **2013**, *48*, 239–250, doi:10.1080/02786826.2013.868596.

72. Zhou, Y.; Wang, T.; Gao, X.; Xue, L.; Wang, X.; Wang, Z.; Gao, J.; Zhang, Q.; Wang, W. Continuous observations of water-soluble ions in PM2.5 at Mount Tai (1534 m a.s.l.) in central-eastern China. *J. Atmos. Chem.* **2009**, *64*, 107–127, doi:10.1007/s10874-010-9172-z.

73. Blanco-Alegre, C.; Calvo, A.I.; Coz, E.; Castro, A.; Oduber, F.; Prevot, A.S.H.; Mocnik, G.; Fraile, R. Quantification of source specific black carbon scavenging using an aethalometer and a disdrometer. *Environ. Pollut.* **2019**, *246*, 336–345, doi:10.1016/j.envpol.2018.11.102.

74. Wang, Z.; Gallet, J.C.; Pedersen, C.A.; Zhang, X.; Strom, J.; Ci, Z. Elemental carbon in snow at Changbai Mountain, northeastern China: concentrations, scavenging ratios, and dry deposition velocities. *Atmos. Chem. Phys.* **2014**, *14*, 629–640, doi:10.5194/acp-14-629-2014.

75. Hegg, D.A.; Clarke, A.D.; Doherty, S.J.; Strom, J. Measurements of black carbon aerosol washout ratio on Svalbard. *Tellus B* **2011**, *63*, 891–900, doi:10.1111/j.1600-0889.2011.00577.x.

76. Xu, J.; Zhang, J.; Liu, J.; Yi, K.; Xiang, S.; Hu, X.; Wang, Y.; Tao, S.; Ban-Weiss, G. Influence of cloud microphysical processes on black carbon wet removal, global distributions, and radiative forcing. *Atmos. Chem. Phys.* **2019**, *19*, 1587–1603, doi:10.5194/acp-19-1587-2019.

77. Gundel, L.A.; Benner, W.H.; Hansen, A.D.A. Chemical-Composition of Fog Water and Interstitial Aerosol in Berkeley, California. *Atmos. Environ.* **1994**, *28*, 2715–2725, doi:10.1016/1352-2310(94)90443-X.

78. Hallberg, A.; Organ, J.A.; Noone, K.J.; Heintenberg, J. Phase partitioning for different aerosol spcies in fog. *Tellus B* **1992**, *44*, 545–555.

79. Gilardoni, S.; Massoli, P.; Giulianelli, L.; Rinaldi, M.; Paglione, M.; Pollini, F.; Lanconelli, C.; Poluzzi, V.; Carbone, S.; Hillamo, R.; et al. Fog scavenging of organic and inorganic aerosol in the Po Valley. *Atmos. Chem. Phys.* **2014**, *14*, 6967–6981, doi:10.5194/acp-14-6967-2014.

80. Hitzenberger, R.; Berner, A.; Kromp, R.; Kasper-Giebl, A.; Limbeck, A.; Tscherwenka, W.; Puxbaum, H. Black carbon and other species at a high-elevation European site (Mount Sonnblick, 3106 m, Austria): Concentrations and scavenging efficiencies. *J. Geophys. Res. Atmos.* **2000**, *105*, 24637–24645, doi:10.1029/2000jd900349.

81. Heintzenberg, J.; Leck, C. Seasonal variation of the atmospheric aerosol near the top of the marine boundary layer over Spitsbergen related to the Arctic sulphur cycle. *Tellus B* **1994**, *46*, 52–67, doi:10.3402/tellusb.v46i1.15751.

82. Wang, X.; Chen, J.; Sun, J.; Li, W.; Yang, L.; Wen, L.; Wang, W.; Wang, X.; Collett, J.L., Jr.; Shi, Y.; et al. Severe haze episodes and seriously polluted fog water in Ji'nan, China. *Sci. Total Environ.* **2014**, *493*, 133–137, doi:10.1016/j.scitotenv.2014.05.135.

83. Gieray, R.; Wieser, P.; Engelhardt, T. Phase partitioning of aerosol constitutents in cloud based on single-particle and bulk analysis. *Atmos. Environ.* **1997**, *31*, 2491–2502.

84. Motos, G.; Schmale, J.; Corbin, J.C.; Modini, R.; Karlen, N.; Bertò, M.; Baltensperger, U.; Gysel, M. Cloud droplet activation properties and scavenged fraction of black carbon in liquid-phase clouds at the high-alpine research station Jungfraujoch (3580 m a.s.l.). *Atmos. Chem. Phys. Discuss.* **2018**, doi:10.5194/acp-2018-1054.

85. Dlugi, R. Chemistry and Deposition of Soot Particles in Moist Air and Fog. *Aerosol Sci. Tech.* **1989**, *10*, 93–105, doi:10.1080/02786828908959224.

86. Collett, J.L., Jr.; Herckes, P.; Youngster, S.; Lee, T. Processing of atmospheric organic matter by California radiation fogs. *Atmos. Res.* **2008**, *87*, 232–241, doi:10.1016/j.atmosres.2007.11.005.

87. Motos, G.; Schmale, J.; Corbin, J.C.; Zanatta, M.; Baltensperger, U.; Gysel, M. Droplet activation behaviour of atmospheric black carbon particles in fog as a function of their size and mixing state. *Atmos. Chem. Phys.* **2019**, *19*, 2183-2207, doi:10.5194/acp-19-2183-2019.

88. Hansen, A.D.A.; Novakov, T. Real-Time Measurements of the Size Fractionation of Ambient Black Carbon Aerosols at Elevated Humidities. *Aerosol Sci. Tech.* **1989**, *10*, 106–110, doi:10.1080/02786828908959225.

89. Chylek, P.; Banic, C.M.; Johnson, B.; Damiano, P.A.; Isaac, G.A.; Leaitch, W.R.; Liu, P.S.K.; Boudala, F.S.; Winter, B.; Ngo, D. Black carbon: Atmospheric concentrations and cloud water content measurements over southern Nova Scotia. *J. Geophys. Res. Atmos.* **1996**, *101*, 29105–29110, doi:10.1029/95jd03433.

90. Hallberg, A.; Ogren, J.A.; Noone, K.J.; Okada, K.; Heintzenberg, J.; Svenningsson, I.B. The Influence of Aerosol-Particle Composition on Cloud Droplet Formation. *J. Atmos. Chem.* **1994**, *19*, 153–171, doi:10.1007/Bf00696587.

91. Schneider, J.; Mertes, S.; van Pinxteren, D.; Herrmann, H.; Borrmann, S. Uptake of nitric acid, ammonia, and organics in orographic clouds: mass spectrometric analyses of droplet residual and interstitial aerosol particles. *Atmos. Chem. Phys.* **2017**, *17*, 1571–1593, doi:10.5194/acp-17-1571-2017.

92. Acker, K.; Mertes, S.; Moller, D.; Wieprecht, W.; Auel, R.; Kalass, D. Case study of cloud physical and chemical processes in low clouds at Mt. Brocken. *Atmos. Res.* **2002**, *64*, 41–51, doi:10.1016/S0169-8095(02)00078-9.

93. Laj, P.; Flossmann, A.I.; Wobrock, W.; Fuzzi, S.; Orsi, G.; Ricci, L.; Mertes, S.; Schwarzenbock, A.; Heintzenberg, J.; Ten Brink, H. Behaviour of H_2O_2, NH_3, and black carbon in mixed-phase clouds during CIME. *Atmos. Res.* **2001**, *58*, 315–336, doi:10.1016/S0169-8095(01)00097-7.

94. Kasper-Giebl, A.; Koch, A.; Hitzenberger, R.; Puxbaum, H. Scavenging efficiency of 'aerosol carbon' and sulfate in supercooled clouds at Mt. Sonnblick (3106m a.s.l., Austria). *J. Atmos. Chem.* **2000**, *35*, 33–46.

95. Moteki, N.; Kondo, Y.; Oshima, N.; Takegawa, N.; Koike, M.; Kita, K.; Matsui, H.; Kajino, M. Size dependence of wet removal of black carbon aerosols during transport from the boundary layer to the free troposphere. *Geophys. Res. Lett.* **2012**, *39*, doi:10.1029/2012GL052034.

96. Matsui, H. Black carbon simulations using a size- and mixing-state-resolved three-dimensional model: 2. Aging timescale and its impact over East Asia. *J. Geophys. Res. Atmos.* **2016**, *121*, 1808–1821, doi:10.1002/2015jd023999.

97. Dusek, U.; Reischl, G.P.; Hitzenberger, R. CCN activation of pure and coated carbon black particles. *Environ. Sci. Technol.* **2006**, *40*, 1223–1230.

98. Ching, J.; West, M.; Riemer, N. Quantifying Impacts of Aerosol Mixing State on Nucleation-Scavenging of Black Carbon Aerosol Particles. *Atmosphere* **2018**, *9*, 17, doi:10.3390/atmos9010017.

99. Dusek, U.; Frank, G.P.; Hildebrandt, L.; Curtius, J.; Schneider, J.; Walter, S.; Chand, D.; Drewnick, F.; Hings, S.; Jung, D.; et al. Size matters more than chemistry for cloud-nucleating ability of aerosol particles. *Science* **2006**, *312*, 1375–1378, doi:10.1126/science.1125261.

100. Shen, Z.; Liu, J.; Horowitz, L.W.; Henze, D.K.; Fan, S.; Levy, H.; Mauzerall, D.L.; Lin, J.; Tao, S. Analysis of transpacific transport of black carbon during HIPPO-3: implications for black carbon aging. *Atmos. Chem. Phys.* **2014**, *14*, 6315–6327, doi:10.5194/acp-14-6315-2014.

101. Zhang, J.; Liu, J.; Tao, S.; Ban-Weiss, G.A. Long-range transport of black carbon to the Pacific Ocean and its dependence on aging timescale. *Atmos. Chem. Phys.* **2015**, *15*, 11521–11535, doi:10.5194/acp-15-11521-2015.

102. He, C.; Li, Q.; Liou, K.N.; Qi, L.; Tao, S.; Schwarz, J.P. Microphysics-based black carbon aging in a global CTM: constraints from HIPPO observations and implications for global black carbon budget. *Atmos. Chem. Phys.* **2016**, *16*, 3077–3098, doi:10.5194/acp-16-3077-2016.

103. Li, K.; Ye, X.; Pang, H.; Lu, X.; Chen, H.; Wang, X.; Yang, X.; Chen, J.; Chen, Y. Temporal variations in the hygroscopicity and mixing state of black carbon aerosols in a polluted megacity area. *Atmos. Chem. Phys.* **2018**, *18*, 15201–15218, doi:10.5194/acp-18-15201-2018.

104. Sarangi, B.; Ramachandran, S.; Rajesh, T.A.; Dhaker, V.K. Black carbon linked aerosol hygroscopic growth: Size and mixing state are crucial. *Atmos. Environ.* **2019**, *200*, 110–118, doi:10.1016/j.atmosenv.2018.12.001.

105. Wittbom, C.; Eriksson, A.C.; Rissler, J.; Carlsson, J.E.; Roldin, P.; Nordin, E.Z.; Nilsson, P.T.; Swietlicki, E.; Pagels, J.H.; Svenningsson, B. Cloud droplet activity changes of soot aerosol upon smog chamber ageing. *Atmos. Chem. Phys.* **2014**, *14*, 9831–9854, doi:10.5194/acp-14-9831-2014.

106. Kupiszewski, P.; Zanatta, M.; Mertes, S.; Vochezer, P.; Lloyd, G.; Schneider, J.; Schenk, L.; Schnaiter, M.; Baltensperger, U.; Weingartner, E.; et al. Ice residual properties in mixed-phase clouds at the high-alpine Jungfraujoch site. *J. Geophys. Res. Atmos.* **2016**, *121*, 12343–12362, doi:10.1002/2016JD024894.

107. Cziczo, D.J.; Froyd, K.D.; Hoose, C.; Jensen, E.J.; Diao, M.; Zondlo, M.A.; Smith, J.B.; Twohy, C.H.; Murphy, D.M. Clarifying the dominant sources and mechanisms of cirrus cloud formation. *Science* **2013**, *340*, 1320–1324, doi:10.1126/science.1234145.

108. Cozic, J.; Mertes, S.; Verheggen, B.; Cziczo, D.J.; Gallavardin, S.J.; Walter, S.; Baltensperger, U.; Weingartner, E. Black carbon enrichment in atmospheric ice particle residuals observed in lower tropospheric mixed phase clouds. *J. Geophys. Res. Atmos.* **2008**, *113*, doi:10.1029/2007jd009266.

109. Targino, A.C.; Coe, H.; Cozic, J.; Crosier, J.; Crawford, I.; Bower, K.; Flynn, M.; Gallagher, M.; Allan, J.; Verheggen, B.; et al. Influence of particle chemical composition on the phase of cold clouds at a high-alpine site in Switzerland. *J. Geophys. Res. Atmos.* **2009**, *114*, doi:10.1029/2008jd011365.

110. Kulkarni, G.; China, S.; Liu, S.; Nandasiri, M.; Sharma, N.; Wilson, J.; Aiken, A.C.; Chand, D.; Laskin, A.; Mazzoleni, C.; et al. Ice nucleation activity of diesel soot particles at cirrus relevant temperature conditions: Effects of hydration, secondary organics coating, soot morphology, and coagulation. *Geophys. Res. Lett.* **2016**, *43*, 3580–3588, doi:10.1002/2016gl068707.

111. Mahmood, R.; von Salzen, K.; Flanner, M.; Sand, M.; Langner, J.; Wang, H.L.; Huang, L. Seasonality of global and Arctic black carbon processes in the Arctic Monitoring and Assessment Programme models. *J. Geophys. Res. Atmos.* **2016**, *121*, 7100–7116, doi:10.1002/2016jd024849.

112. Liu, D.; Flynn, M.; Gysel, M.; Targino, A.; Crawford, I.; Bower, K.; Choularton, T.; Juranyi, Z.; Steinbacher, M.; Huglin, C.; et al. Single particle characterization of black carbon aerosols at a tropospheric alpine site in Switzerland. *Atmos. Chem. Phys.* **2010**, *10*, 7389–7407, doi:10.5194/acp-10-7389-2010.

113. Ducret, J.; Cachier, H. Particulate Carbon Content in Rain at Various Temperate and Tropical Locations. *J. Atmos. Chem.* **1992**, *15*, 55–67, doi:10.1007/Bf00053609.

114. Cerqueira, M.; Pio, C.; Legrand, M.; Puxbaum, H.; Kasper-Giebl, A.; Afonso, J.; Preunkert, S.; Gelencser, A.; Fialho, P. Particulate carbon in precipitation at European background sites. *J. Aerosol Sci.* **2010**, *41*, 51–61, doi:10.1016/j.jaerosci.2009.08.002.

115. Tsyro, S.; Simpson, D.; Tarrason, L.; Klimont, Z.; Kupiainen, K.; Pio, C.; Yttri, K.E. Modeling of elemental carbon over Europe. *J. Geophys. Res. Atmos.* **2007**, *112*, doi:10.1029/2006jd008164.

116. Gogoi, M.M.; Babu, S.S.; Moorthy, K.K.; Thakur, R.C.; Chaubey, J.P.; Nair, V.S. Aerosol black carbon over Svalbard regions of Arctic. *Polar Sci.* **2016**, *10*, 60–70, doi:10.1016/j.polar.2015.11.001.

117. Gogoi, M.M.; Babu, S.S.; Pandey, S.K.; Nair, V.S.; Vaishya, A.; Girach, I.A.; Koushik, N. Scavenging ratio of black carbon in the Arctic and the Antarctic. *Polar Sci.* **2018**, *16*, 10–22, doi:10.1016/j.polar.2018.03.002.

118. Grythe, H.; Kristiansen, N.I.; Zwaaftink, C.D.G.; Eckhardt, S.; Strom, J.; Tunved, P.; Krejci, R.; Stohl, A. A new aerosol wet removal scheme for the Lagrangian particle model FLEXPART v10. *Geosci. Model Dev.* **2017**, *10*, 1447–1466, doi:10.5194/gmd-10-1447-2017.

119. Zhang, L.; Michelangeli, D.V.; Taylor, P.A. Numerical studies of aerosol scavenging by low-level, warm stratiform clouds and precipitation. *Atmos. Environ.* **2004**, *38*, 4653–4665, doi:10.1016/j.atmosenv.2004.05.042.

120. Levin, Z.; Teller, A.; Ganor, E.; Graham, B.; Andreae, M.O.; Maenhaut, W.; Falkovich, A.H.; Rudich, Y. Role of aerosol size and composition in nucleation scavenging within clouds in a shallow cold front. *J. Geophys. Res. Atmos.* **2003**, *108*, doi:10.1029/2003jd003647.

121. Andronache, C. Estimated variability of below-cloud aerosol removal by rainfall for observed aerosol size distributions. *Atmos. Chem. Phys.* **2003**, *3*, 131–143, doi:10.5194/acp-3-131-2003.

122. Kondo, Y.; Moteki, N.; Oshima, N.; Ohata, S.; Koike, M.; Shibano, Y.; Takegawa, N.; Kita, K. Effects of wet deposition on the abundance and size distribution of black carbon in East Asia. *J. Geophys. Res. Atmos.* **2016**, *121*, 4691–4712, doi:10.1002/2015jd024479.

123. Emerson, E.W.; Katich, J.M.; Schwarz, J.P.; McMeeking, G.R.; Farmer, D.K. Direct Measurements of Dry and Wet Deposition of Black Carbon Over a Grassland. *J. Geophys. Res. Atmos.* **2018**, *123*, 12277–12290, doi:10.1029/2018jd028954.

124. Budhavant, K.B.; Rao, P.S.P.; Safai, P.D.; Leck, C.; Rodhe, H. Black carbon in cloud-water and rain water during monsoon season at a high altitude station in India. *Atmos. Environ.* **2016**, *129*, 256–264, doi:10.1016/j.atmosenv.2016.01.028.

125. Kanaya, Y.; Pan, X.; Miyakawa, T.; Komazaki, Y.; Taketani, F.; Uno, I.; Kondo, Y. Long-term observations of black carbon mass concentrations at Fukue Island, western Japan, during 2009–2015: Constraining wet removal rates and emission strengths from East Asia. *Atmos. Chem. Phys.* **2016**, *16*, 10689–10705, doi:10.5194/acp-16-10689-2016.

126. Huo, M.Q.; Sato, K.; Ohizumi, T.; Akimoto, H.; Takahashi, K. Characteristics of carbonaceous components in precipitation and atmospheric particle at Japanese sites. *Atmos. Environ.* **2016**, *146*, 164–173, doi:10.1016/j.atmosenv.2016.07.017.

127. Andronache, C.; Gronholm, T.; Laakso, L.; Phillips, V.; Venalainen, A. Scavenging of ultrafine particles by rainfall at a boreal site: observations and model estimations. *Atmos. Chem. Phys.* **2006**, *6*, 4739–4754, doi:10.5194/acp-6-4739-2006.

128. Wu, Z.; Hu, M.; Lin, P.; Liu, S.; Wehner, B.; Wiedensohler, A. Particle number size distribution in the urban atmosphere of Beijing, China. *Atmos. Environ.* **2008**, *42*, 7967–7980, doi:10.1016/j.atmosenv.2008.06.022.

129. Bae, S.Y.; Park, R.J.; Kim, Y.P.; Woo, J.H. Effects of below-cloud scavenging on the regional aerosol budget in East Asia. *Atmos. Environ.* **2012**, *58*, 14–22, doi:10.1016/j.atmosenv.2011.08.065.

130. Querel, A.; Monier, M.; Flossmann, A.I.; Lemaitre, P.; Porcheron, E. The importance of new collection efficiency values including the effect of rear capture for the below-cloud scavenging of aerosol particles. *Atmos. Res.* **2014**, *142*, 57–66, doi:10.1016/j.atmosres.2013.06.008.

131. Zhao, S.; Yu, Y.; He, J.; Yin, D.; Wang, B. Below-cloud scavenging of aerosol particles by precipitation in a typical valley city, northwestern China. *Atmos. Environ.* **2015**, *102*, 70–78, doi:10.1016/j.atmosenv.2014.11.051.

132. Seland, O.; Iversen, T. A scheme for black carbon and sulphate aerosols tested in a hemispheric scale, Eulerian dispersion model. *Atmos. Environ.* **1999**, *33*, 2853–2879, doi:10.1016/S1352-2310(98)00389-6.

133. Hou, P.; Wu, S.; McCarty, J.L.; Gao, Y. Sensitivity of atmospheric aerosol scavenging to precipitation intensity and frequency in the context of global climate change. *Atmos. Chem. Phys.* **2018**, *18*, 8173–8182, doi:10.5194/acp-18-8173-2018.

134. Witkowska, A.; Lewandowska, A.; Falkowska, L.M. Parallel measurements of organic and elemental carbon dry (PM_1, $PM_{2.5}$) and wet (rain, snow, mixed) deposition into the Baltic Sea. *Mar. Pollut. Bull.* **2016**, *104*, 303–312, doi:10.1016/j.marpolbul.2016.01.003.

135. Oshima, N.; Kondo, Y.; Moteki, N.; Takegawa, N.; Koike, M.; Kita, K.; Matsui, H.; Kajino, M.; Nakamura, H.; Jung, J.S.; et al. Wet removal of black carbon in Asian outflow: Aerosol Radiative Forcing in East Asia (A-FORCE) aircraft campaign. *J. Geophys. Res. Atmos.* **2012**, *117*, doi:10.1029/2011jd016552.

136. Girach, I.A.; Nair, V.S.; Babu, S.S.; Nair, P.R. Black carbon and carbon monoxide over Bay of Bengal during W_ICARB: Source characteristics. *Atmos. Environ.* **2014**, *94*, 508–517, doi:10.1016/j.atmosenv.2014.05.054.

137. Latha, K.M.; Badarinath, K.V.S.; Reddy, P.M. Scavenging efficiency of rainfall on black carbon aerosols over an urban environment. *Atmos. Sci. Lett.* **2005**, *6*, 148–151, doi:10.1002/asl.108.

138. Hoose, C.; Lohmann, U.; Stier, P.; Verheggen, B.; Weingartner, E. Aerosol processing in mixed-phase clouds in ECHAM5-HAM: Model description and comparison to observations. *J. Geophys. Res. Atmos.* **2008**, *113*, doi:10.1029/2007jd009251.

139. Koch, D.; Schulz, M.; Kinne, S.; McNaughton, C.; Spackman, J.R.; Balkanski, Y.; Bauer, S.; Berntsen, T.; Bond, T.C.; Boucher, O.; et al. Evaluation of black carbon estimations in global aerosol models. *Atmos. Chem. Phys.* **2009**, *9*, 9001–9026, doi:10.5194/acp-9-9001-2009.

140. Samset, B.H.; Myhre, G.; Herber, A.; Kondo, Y.; Li, S.; Moteki, N.; Koike, M.; Oshima, N.; Schwarz, J.P.; Balkanski, Y.; et al. Modelled black carbon radiative forcing and atmospheric lifetime in AeroCom Phase II constrained by aircraft observations. *Atmos. Chem. Phys.* **2014**, *14*, 12465–12477, doi:10.5194/acp-14-12465-2014.

141. Iversen, T. A scheme for process-tagged SO4 and BC aerosols in NCAR CCM3: Validation and sensitivity to cloud processes. *J. Geophys. Res. Atmos.* **2002**, *107*, doi:10.1029/2001jd000885.

142. Srivastava, R.; Bran, S.H. Impact of dynamical and microphysical schemes on black carbon prediction in a regional climate model over India. *Environ. Sci. Pollut. Res. Int.* **2018**, *25*, 14844–14855, doi:10.1007/s11356-018-1607-0.

143. Huang, Y.; Chameides, W.L.; Tan, Q.; Dickinson, R.E. Characteristics of Anthropogenic Sulfate and Carbonaceous Aerosols over East Asia: Regional Modeling and Observation. *Adv. Atmos. Sci.* **2008**, *25*, 946–959, doi:10.1007/s00376-008-0946-z.

144. Koch, D. Transport and direct radiative forcing of carbonaceous and sulfate aerosols in the GISS GCM. *J. Geophys. Res. Atmos.* **2001**, *106*, 20311–20332, doi:10.1029/2001jd900038.

145. Kipling, Z.; Stier, P.; Schwarz, J.P.; Perring, A.E.; Spackman, J.R.; Mann, G.W.; Johnson, C.E.; Telford, P.J. Constraints on aerosol processes in climate models from vertically-resolved aircraft observations of black carbon. *Atmos. Chem. Phys.* **2013**, *13*, 5969–5986, doi:10.5194/acp-13-5969-2013.

146. Pierce, J.R.; Croft, B.; Kodros, J.K.; D'Andrea, S.D.; Martin, R.V. The importance of interstitial particle scavenging by cloud droplets in shaping the remote aerosol size distribution and global aerosol-climate effects. *Atmos. Chem. Phys.* **2015**, *15*, 6147–6158, doi:10.5194/acp-15-6147-2015.

147. Croft, B.; Lohmann, U.; Martin, R.V.; Stier, P.; Wurzler, S.; Feichter, J.; Hoose, C.; Heikkila, U.; van Donkelaar, A.; Ferrachat, S. Influences of in-cloud aerosol scavenging parameterizations on aerosol

concentrations and wet deposition in ECHAM5-HAM. *Atmos. Chem. Phys.* **2010**, *10*, 1511–1543, doi:10.5194/acp-10-1511-2010.

148. Yang, Q.; Gustafson, W.I.; Fast, J.D.; Wang, H.; Easter, R.C.; Morrison, H.; Lee, Y.N.; Chapman, E.G.; Spak, S.N.; Mena-Carrasco, M.A. Assessing regional scale predictions of aerosols, marine stratocumulus, and their interactions during VOCALS-REx using WRF-Chem. *Atmos. Chem. Phys.* **2011**, *11*, 11951–11975, doi:10.5194/acp-11-11951-2011.

149. Thomas, J.L.; Polashenski, C.M.; Soja, A.J.; Marelle, L.; Casey, K.A.; Choi, H.D.; Raut, J.C.; Wiedinmyer, C.; Emmons, L.K.; Fast, J.D.; et al. Quantifying black carbon deposition over the Greenland ice sheet from forest fires in Canada. *Geophys. Res. Lett.* **2017**, *44*, 7965–7974, doi:10.1002/2017gl073701.

150. Hienola, A.I.; Pietikäinen, J.P.; Jacob, D.; Pozdun, R.; Petäjä, T.; Hyvärinen, A.P.; Sogacheva, L.; Kerminen, V.M.; Kulmala, M.; Laaksonen, A. Black carbon concentration and deposition estimations in Finland by the regional aerosol–climate model REMO-HAM. *Atmos. Chem. Phys.* **2013**, *13*, 4033–4055, doi:10.5194/acp-13-4033-2013.

151. Stier, P.; Feichter, J.; Kinne, S.; Kloster, S.; Vignati, E.; Wilson, J.; Ganzeveld, L.; Tegen, I.; Werner, M.; Balkanski, Y.; et al. The aerosol-climate model ECHAM5-HAM. *Atmos. Chem. Phys.* **2005**, *5*, 1125–1156, doi:10.5194/acp-5-1125-2005.

152. Yang, Q.; Gustafson, W.I.; Fast, J.D.; Wang, H.; Easter, R.C.; Wang, M.; Ghan, S.J.; Berg, L.K.; Leung, L.R.; Morrison, H. Impact of natural and anthropogenic aerosols on stratocumulus and precipitation in the Southeast Pacific: a regional modelling study using WRF-Chem. *Atmos. Chem. Phys.* **2012**, *12*, 8777–8796, doi:10.5194/acp-12-8777-2012.

153. Fan, S.-M.; Schwarz, J.P.; Liu, J.; Fahey, D.W.; Ginoux, P.; Horowitz, L.W.; Levy, H.; Ming, Y.; Spackman, J.R. Inferring ice formation processes from global-scale black carbon profiles observed in the remote atmosphere and model simulations. *J. Geophys. Res. Atmos.* **2012**, *117*, D23205, doi:10.1029/2012jd018126.

154. Ching, J.; Riemer, N.; West, M. Impacts of black carbon mixing state on black carbon nucleation scavenging: Insights from a particle-resolved model. *J. Geophys. Res. Atmos.* **2012**, *117*, doi:10.1029/2012jd018269.

155. Lund, M.T.; Berntsen, T.K.; Samset, B.H. Sensitivity of black carbon concentrations and climate impact to aging and scavenging in OsloCTM2–M7. *Atmos. Chem. Phys.* **2017**, *17*, 6003–6022, doi:10.5194/acp-17-6003-2017.

156. Gong, X.; Zhang, C.; Chen, H.; Nizkorodov, S.A.; Chen, J.; Yang, X. Size distribution and mixing state of black carbon particles during a heavy air pollution episode in Shanghai. *Atmos. Chem. Phys.* **2016**, *16*, 5399–5411, doi:10.5194/acp-16-5399-2016.

157. Hitzenberger, R.; Tohno, S. Comparison of black carbon (BC) aerosols in two urban areas—Concentrations and size distributions. *Atmos. Environ.* **2001**, *35*, 2153–2167.

158. Safai, P.D.; Raju, M.P.; Budhavant, K.B.; Rao, P.S.P.; Devara, P.C.S. Long term studies on characteristics of black carbon aerosols over a tropical urban station Pune, India. *Atmos. Res.* **2013**, *132*, 173–184, doi:10.1016/j.atmosres.2013.05.002.

159. Wu, Y.; Cheng, T.; Liu, D.; Allan, J.D.; Zheng, L.; Chen, H. Light Absorption Enhancement of Black Carbon Aerosol Constrained by Particle Morphology. *Environ. Sci. Technol.* **2018**, *52*, 6912–6919, doi:10.1021/acs.est.8b00636.

160. Adachi, K.; Chung, S.H.; Buseck, P.R. Shapes of soot aerosol particles and implications for their effects on climate. *J. Geophys. Res. Atmos.* **2010**, *115*, doi:10.1029/2009jd012868.

161. Li, W.; Shao, L.; Zhang, D.; Ro, C.; Hu, M.; Bi, X.; Geng, H.; Matsuki, A.; Niu, H.; Chen, J. A review of single aerosol particle studies in the atmosphere of East Asia: morphology, mixing state, source, and heterogeneous reactions. *J. Clean. Prod.* **2016**, *112*, 1330–1349, doi:10.1016/j.jclepro.2015.04.050.

162. Ueda, S.; Osada, K.; Okada, K. Mixing states of cloud interstitial particles between water-soluble and insoluble materials at Mt. Tateyama, Japan: Effects of meteorological conditions. *Atmos. Res.* **2011**, *99*, 325–336, doi:10.1016/j.atmosres.2010.10.021.

163. Croft, B.; Martin, R.V.; Leaitch, W.R.; Tunved, P.; Breider, T.J.; D'Andrea, S.D.; Pierce, J.R. Processes controlling the annual cycle of Arctic aerosol number and size distributions. *Atmos. Chem. Phys.* **2016**, *16*, 3665–3682, doi:10.5194/acp-16-3665-2016.

164. Yin, J.; Wang, D.; Zhai, G.; Xu, H. An investigation into the relationship between liquid water content and cloud number concentration in the stratiform clouds over north China. *Atmos. Res.* **2014**, *139*, 137–143, doi:10.1016/j.atmosres.2013.12.004.

165. Koracin, D.; Businger, J.; Dorman, C.; Lewis, J. Formation, evolution, and dissipation of coastal sea fog. *Bound.-Layer Meteorol.* **2005**, *117*, 447–478, doi:10.1007/s10546-005-2772-5.

166. Dupont, J.-C.; Haeffelin, M.; Protat, A.; Bouniol, D.; Boyouk, N.; Morille, Y. Stratus–Fog Formation and Dissipation: A 6-Day Case Study. *Bound.-Layer Meteorol.* **2012**, *143*, 207–225, doi:10.1007/s10546-012-9699-4.

167. Targino, A.C.; Noone, K.J.; Drewnick, F.; Schneider, J.; Krejci, R.; Olivares, G.; Hings, S.; Borrmann, S. Microphysical and chemical characteristics of cloud droplet residuals and interstitial particles in continental stratocumulus clouds. *Atmos. Res.* **2007**, *86*, 225–240, doi:10.1016/j.atmosres.2007.05.001.